Cycle configuration analysis and techno-economic sensitivity of biomass externally fired gas turbine with bottoming ORC

CYCLE CONFIGURATION ANALYSIS AND TECHNO-ECONOMIC SENSITIVITY OF BIOMASS EXTERNALLY FIRED GAS TURBINE WITH BOTTOMING ORC

Sergio M Camporeale[1], Antonio M Pantaleo[2,*], Patrizia D Ciliberti[1], Bernardo Fortunato[1]

[1]Politecnico di Bari, Department of Mechanics, Mathematics and Management, (DMMM), Via Orabona 4, Bari 70125, Italy

[2]Imperial College London, Centre for Energy Policy and Technology, South Ken Campus, 7SW 2 AZ London UK and Università degli studi di Bari Aldo Moro, Department of agro-environmental sciences, Via Amendola 165/A – Bari – 70125

* corresponding author: a.pantaleo@imperial.ac.uk; antonio.pantaleo@uniba.it;

ABSTRACT

This paper focuses on the energy analysis of a combined cycle composed by a topping 1.3 MW Externally Fired Gas Turbine (EFGT) with direct combustion of biomass and a bottoming Organic Rankine Cycle (ORC). A non recuperative scheme is assumed for the EFGT in order to avoid the costs of the recuperator. This scheme presents lower conversion efficiency in comparison to a recuperative one, however the heat available for the bottoming cycle is at a higher temperature (about 400°C). In the present work, evaporation pressure and superheating temperature of ORC cycle are ranged in order to examine different bottoming cycles, including supercritical ones. Different organic fluids are investigated, such as siloxanes and toluene, aiming to analyze how the fluid choice influences both the plant performance and important features for the ORC turbine design. On the basis of the results of the thermodynamic simulation, a thermo-economic assessment is proposed, to investigate the profitability of the bottoming ORC in comparison to only topping EFGT, and the most influencing techno-economic factors that influence the selection of the optimal cycle. In order to propose real case studies, the Italian bioenergy subsidy framework is assumed, and the sensitivity assessment includes the options of only electricity and CHP, at different biomass cost, thermal energy demand and heat selling price values.

KEYWORDS

EFGT, ORC, microturbine, biomass, siloxanes

HIGHLIGHTS

- a methodology to design the bottoming ORC cycle coupled to a biomass fired EFGT is proposed

- the influence of cycle thermodynamic parameters in the ORC turbine design is investigated
- the fluid selection affects more the heat recovery ratio (in CHP configuration) than the combined cycle conversion efficiency
- Bottoming ORC results a promising option to increase conversion efficiency and profitability of EFGT
- energy demand characteristics (temperature of heat demand and energy intensity) are key factors for the selection of the optimal cycle configuration

1. INTRODUCTION

In the European Union, the European Commission (EC) Decision [1] has defined the GHG emission limits by 2020 compared to 2005 levels for each Member State (MS), in order to reduce GHGs of 20% on respect to 1990 levels. Heat and power generation from Renewable Energy Sources (RES) is recognized as a particularly important means of reducing GHG emissions [2].

In particular, small scale and on site CHP plants operated within ESCO (Energy Service Company) schemes can be promising for the residential and tertiary sector, which are commonly affected by high energy demand intensity and costs, and for the industrial sector, in particular in case of energy-intensive processes, concurrent heat and power demand, and high tariffs of electricity and heating [3]. The use of biomass in small scale CHP plants has been widely investigated in literature, including, among the others, topics such as biomass upgrading and processing technologies, logistics of supply, optimization of CHP plants sizing, location and operation. In the field of energy conversion of lignocellulosic biomass, the available technologies for small scale CHP (100 kWe to 1 MWe size) include two main options: (i) biomass pre-processing through gasification and (ii) direct combustion in grate or fluidized bed boilers. In this second option, externally fired MGT [4,5], Stirling engines [6,7] and Organic Rankine Cycles (ORC) [8,9] are largely investigated as technically viable alternatives to steam plants in order to efficiently convert the heat produced by the biomass combustion. An assessment of small scale biomass CHP plants including steam vs ORC plants in different energy demand segments is given in [10]. The application of dual fuel schemes (direct biomass combustion and natural gas) in order to improve the efficiency of MGT has been examined in [11,12], while in [13] the technical and economical aspects related to the part load performance are examined.

Research on EFGT systems has considerably increased during last years, especially in configuration fired by biomass. In [14], a Aspen Plus and Matlab based simulation of EFGT coupled to syngas from biomass gasification is proposed, in order to explore the influence of fuel quality, dual fuel operation (natural gas mix) and other thermodynamic parameters on cycle performance. Other

studies [15–17] focus on methods to increase the efficiency both in simple cycle and in combined cycle configurations, investigating the use of metallic as well as ceramic materials for high temperature heat exchangers. Another configuration capable of enhancing the power output and efficiency of the EFGT, by increasing the mass flow through the turbine, the so called externally fired humid air turbine (EFHAT), is proposed in [18,19].

In [20], a small scale double shaft intercooled EFGT cycle is investigated, assuming a 50 kW biomass system with a grate combustor boiler and turbine inlet temperature of 750 °C. A preliminary sizing of the high temperature heat exchanger is performed, while the potential advantages of this externally fired configuration with respect to the existing technologies are discussed on the basis of numerical simulations in other works [21-22].

On the other side, a number of researches aimed to quantify the benefits of ORC bottoming cycles coupled to MGT [23-26]. In particular, in [23,26], a modified recuperative micro gas turbine is proposed in order to perform an externally fired scheme with direct combustion of biomass. This scheme, assuming a turbine inlet temperature of 900°C, coupled to an optimized bottoming ORC cycle is expected to reach an electric efficiency of 23.5% with respect to 19.2% of the EFGT alone.

In [27] an interesting scheme for a small size gas turbine (1.3 MW of electric power) is proposed. An intercooled non recuperative cycle is considered with direct biomass combustion. Although this cycle has a relatively poor efficiency, the costs of investment per kW are lower on respect to a recuperative cycle because of the absence of the recuperator. Other interesting features are: higher specific work that determinates lower investment cost per kW, higher pressure ratio that allows for easier and more economic design of the heat exchangers of the air circuit. Due to the higher pressure ratio, the sensitivity of the cycle efficiency to pressure losses in the heat exchangers is much lower than in a recuperative cycle.

In the domain of thermo-economic assessment of energy conversion systems, several methodologies have been proposed in literature, as reviewed in [11], focusing on a number of renewable sources [49,50], a wide range of end user typologies [51,52], including residential, tertiary and industrial sectors, and a broad range of energy management strategies for the optimal system operation [53,54,55].

In the proposed research, a thermodynamic analysis of the bottoming ORC cycle is carried out in order to evaluate how the lower efficiency of the topping cycle can be compensated by an efficient bottoming cycle. The thermodynamic analysis is focused on the selection of the optimal design point for a given ORC fluid and on a comparison among different fluids. The ORC is much more suited than conventional steam turbines for small and micro CHP plants from a few dozen to some hundreds kWe. In facts, instead of water, ORC uses organic chemicals with favorable

thermodynamic properties as working fluids so that the enthalpy drop is much lower and the flow can be expanded in a turbine by means of few stages.

The selection of the working fluid is a relevant issue in the ORC design. This selection is based on the temperature of heat sources and on environmental and safety regulations. In particular, refrigerant can be used for low temperatures (100-180°C), hydrocarbons for middle temperatures (200-180°C), while siloxanes and toluene are suitable for higher temperature (250-350°C) [28].

The fluids can be classified as wet, dry and isentropic ones on the basis of the slope of the saturated vapor curve (dS/dT). Isentropic and dry fluids are preferred for ORC applications since they ensure a dry expansion avoiding droplet formation that can damage turbine blades, and allowing for saturated, subcritical or supercritical cycles. A review of ORC fluid selection has been proposed in a number of researches [29,30], nevertheless the selection of the best working fluid for a new application is still a difficult task.

The working fluid also influences the turbine design parameters (speed of revolution, number of stages, dimensions) and, in turn, its performance. The size parameter S_p and the volume expansion ratio V_r are often used for the turbine design. Macchi [31] suggests the use of efficiency prediction maps based on both V_r and S_P, both for single stage and double stage axial turbines. Moreover, different layout schemes could be adopted [32].

In the last section, following the methodology described in [11], a thermo-economic assessment is proposed, comparing the profitability of the EFGT with and without the bottoming ORC. The main advantage of the bottoming ORC is to increase the electric conversion efficiency, having as drawback higher upfront cost and lower temperature of heat available for cogeneration.

A baseload operating strategy, feeding electricity directly into the grid, is here assumed, being this typology of CHP plants eligible for feed-in tariffs in the Italian energy market [12], while other operating strategies, such as the option of thermal or electric demand following, are addressed in [10,13].

2. THERMODYNAMIC ANALYSIS

The aim of the first part of the paper is the thermodynamic analysis of the combined cycle composed by an External Fired Gas Turbine – EFGT - and an Organic Rankine Cycle –ORC. The plant layout of the combined cycle is shown in Figure 1 while Figure 2 shows the T-s diagram of the cycle. The software for simulation is Cycle-Tempo [33] and the thermodynamic properties are obtained from FluidProp library [33].

The topping cycle is an inter-refrigerated gas turbine, with direct combustion of biomass (C 50%, H_2 6%, O_2 44%, 40% of humidity). The heat of the hot gas produced in the furnace is transferred to

the air flowing in the gas turbine through a heat exchanger (D-E) placed between the inter-refrigerated compressor (A-D) and the turbine (E-F), as reported in Fig 1. Table 1 summarizes the design values of the EFGT. Following [34], a TIT of 800°C is assumed, and this low temperature allows a quite low cost for the heat exchanger steel.

Figure 1 – EFGT-ORC Combined Cycle Plant Layout

Figure 2 - T-s chart. EFGT-ORC Combined Cycle.

In the conventional EFGT scheme the biomass is fed to an external furnace together with hot air coming from the turbine exhaust, however in this work, as proposed in [11, 34], combustion air is taken from ambient. This configuration allows for a more flexible regulation, since the circuit of the working air flowing in the turbine and that one of the combustion air flowing in the furnace are independent. Furthermore, the gas exiting the turbine is pure air, without impurities coming from combustion. For combined cycles and/or cogeneration, this is an important feature since it allows the hot gas exiting from the turbine to be cooled to low temperature, hence avoiding the problems related to the condensation of hot gas produced by the biomass combustion.

From our calculations, the electric power output is 1,383 kW and the thermal flow from the exhaust gas is 4,083 kW at the temperature of 394°C.

The bottoming cycle is composed by an ORC in recuperative configuration, with the adoption of a Recuperative Heat Exchanger (RHE) (or "recuperator") and a "dry" fluid. . In particular, the cycle (see the plant layout in Figure 1) contains a pump (6-1) that supplies the organic fluid to the RHE. The RHE pre-heats the working fluid (1-2) using the thermal energy coming from desuperheating process of the organic fluid before entering the condenser.

The Heat Recovery Boiler (HRB) completes the evaporation (2-3) by means of heat recovered from the topping cycle. In general, the HRB is composed by an economizer that heats the fluids up to the evaporation temperature, an evaporator for a complete evaporation of the fluid and a superheater (in superheated cycles). The vapor exiting the HRB flows across the turbine (3-4), then to the hot side of the RHE (4-5), and finally to the condenser (5-6).

Table 1 –Main calculation hypotheses for the EFGT cycle

In the T-s diagram of the combined cycle EFGT+ORC of Figure 2, the temperature T_G at the HRB exit is the stack temperature and is related to the temperature T_2 of the organic fluid at the cold side regenerator exit. The choice of the regenerative scheme for the bottoming cycle is discussed in the

next section. Considering that the EFGT turbine outlet temperature is 394°C, siloxanes and toluene are suitable working fluids for the ORC cycle. In particular, hexamethyldisiloxane –MM- is firstly examined. Since the critical pressure of MM is of 19.39 bar, subcritical cycles are examined, ranging the evaporation pressure from 1 bar to 19 bar. Supercritical cycles are then examined, ranging the evaporation pressure from 20 to 25 bar. For each value of evaporation pressure, superheated cycles up to a maximum temperature of 390°C are examined. The T-s diagrams of the bottoming ORC in the different cases are shown in

Figure 3. A saturated cycle is reproduced in Figure 2(a); two superheated cycles are shown in Figure 2(b) and 2(c), with two different evaporation pressures; finally, a supercritical cycle is shown in Figure 2(d). The condensation temperature of 40°C and the other parameters, summarized in Table 2 are unchanged in the present thermodynamic analysis. T-Q diagrams of the HRB for the four cycles of
Figure 3, are shown in Figure 4.

Figure 3 – T-s chart for some examined cases: a) p_{ev}=5 bar, saturated; b) p_{ev}=5 bar, T_3=260°C; c) p_{ev}=10 bar, T_3=260°C; d) supercritical cycle p_{ev}=25 bar, T_3= 270°C

Figure 4 –T-Q diagrams for the HRB. Cases (a) to (d).

The thermodynamic analysis of the combined cycle is carried out under the hypothesis that the bottoming cycle does not influence the performance of the topping cycle. Actually, the backpressure at the exit of the EFGT is influenced by the pressure losses across the HRB. However, in this work, those pressure losses are considered constant, so that efficiency, power output and exhaust gas temperature are assumed constant.

Following [48], the energy performance of the bottoming cycle are evaluated from: (i) the "internal thermal efficiency of the bottoming cycle", η_L, defined as the ratio between the power output of the bottoming cycle $P_{e,ORC}$, , and the input heat flux to the bottoming cycle, $\dot{Q}_L$, (i.e. the heat recovered in the HRB); (ii) the "heat recovery ratio" or "heat recovery boiler efficiency" χ , defined as the ratio between heat recovered $\dot{Q}_L$, and heat flux made available to the bottoming cycle, $\dot{Q}_{av}$

$$\eta_L = \frac{P_{e,ORC}}{\dot{Q}_L} \tag{1}$$

$$\chi = \frac{\dot{Q}_L}{\dot{Q}_{av}} \tag{2}$$

The heat flux

$$\dot{Q}_L = \dot{m}_g \, c_{p,g}(T_{\mathrm{F}} - T_G) \tag{3}$$

$$\dot{Q}_{av} = \dot{m}_g \, c_{p,g}(T_F - T_{\mathrm{amb}}) \tag{4}$$

The "overall efficiency of the bottoming cycle", η_{rec} is defined as the ratio between the power output of the bottoming cycle and the heat flux available from the topping cycle. Then, according to Eq.(1) and (2), it results

$$\eta_{rec} = \frac{P_{e,ORC}}{\dot{Q}_{av}} = \chi \cdot \eta_L . \tag{5}$$

The modifications of the bottoming cycle do not influence the topping cycle, excepted for the backpressure variation at the turbine exit, that influences the turbine power output. Neglecting such influence, from Eq.(5) it follows that the maximum power output for the combined cycle is obtained under the condition that maximizes the product of η_L and χ.

Finally, the combined cycle efficiency is given by Eq (6), where $P_{e,\mathrm{EFGT}}$ is the power output of the topping cycle (EFGT), $\dot{m}_b$ is the biomass flow and LHV is lower heating value of biomass.

$$\eta_{cc} = \frac{P_{e,EFGT} + P_{e,ORC}}{\dot{m}_b \, LHV}. \tag{6}$$

Table 2- Basic assumptions for ORC calculation

2.1 Influence of evaporation pressure and superheating temperature

Subcritical cycles are first examined, varying the evaporation pressure from 1 bar to 19 bar, including saturated cycles (

Figure 3(a)) and superheated cycles with superheating temperature up to 390°C (

Figure 3(b-c)). The performance of these cycles, represented by η_L, χ and η_{rec} are shown in Figure 5 as function of the maximum cycle temperature T_3, that is the ORC Turbine Inlet Temperature (TIT), and for different values of the evaporation pressure, p_{ev}. The internal efficiency η_L, of saturated cycles is always increasing with evaporation pressure. For superheated cycles, the internal efficiency η_L increases with evaporation pressure and superheating temperature. This result is coherent with the characteristics of the bottoming cycle that is a recuperative cycle. In fact, as shown in

Figure 3, when increasing the evaporation pressure p_{ev} and the max cycle temperature T_3, the heat input to the bottoming cycle occurs within higher temperatures.

The efficiency η_L of supercritical cycles with evaporation pressure of 20 and 25 bar, is also plotted in Figure 5(a). The plots at higher pressures are not given for sake of clarity. It results that η_L is always increasing with pressure and cycle max temperature.

The heat flux recovered in the HRB, $\dot{Q}_L$, and the corresponding heat recovery ratio χ are plotted in Figure 5 (b). It appears that, in the case of saturated cycles, the heat flux recovered is always decreasing with the evaporation pressure., as resulting from the Q-T diagram for a saturated cycle, reported in Figure 4(a). , which also indicates the pinch constraint at the cold end of the HRB. This entails that, when increasing the superheated vapor temperature, the feed temperature T_2 of the liquid to the HRB also increases, due to heat recuperation in the RHE. Hence, the temperature T_G of the gas exiting the HRB increases and, finally, the heat recovery ratio χ decreases.

Figure 5- Effect of ORC Turbine Inlet Temperature and Evaporation Pressure on a) internal ORC cycle thermal efficiency, η_L ; b) heat exchanged in the HRB and heat recovery ratio; c) electric power output and overall efficiency of the ORC cycle, η_{rec}, for subcritical (1 to 19 bar) and supercritical (20 to 25 bar) cycles

For superheated cycles, the graphs of the heat recovery ratio χ show three different trends (see graphs for evaporation pressures 4 to 16 bars in **Figure 5** (b)):

(i) In the first segment, the heat recovery ratio is decreasing with the superheating temperature. This can be justified if one observes Figure 4(b) and (c) that show the T-Q plot of the HRB. It appears that pinch occurs at the cold end of the HRB; therefore, when increasing the superheated temperature, due to the recuperator, the feed temperature of the organic fluid to the HRB is increased. Consequently, the temperature of the gas exiting the HRB increases and, finally, the heat recovery ratio is lowered.

(ii) In the second segment, the heat flux needed for vaporization is partly transferred in the internal recuperator RHE. Consequently, the pinch constraint in the T-Q diagram of the HRB occurs at the evaporation temperature (see Figure 4 (b)). Therefore, even if the temperature the ORC turbine inlet temperature T_3, increases, the stack temperature T_G remains constant, as well as the heat recovery ratio.

(iii) In third segment, the heat flux needed for vaporization is entirely recovered in the internal recuperator. Consequently, the HRB supplies heat only for superheating. As in the case (i), the stack temperature T_G increases with T_3 and the heat recovery ratio χ is lowered.

For supercritical cycles (graphs for evaporation pressures 20 and 25 bar) the heat recovery ratio χ is always decreasing with the temperature T_3. The T-Q diagram of the HRB given in Figure 4 (d)

corresponding to one of the case at 25 bar, shows the pinch constraint at the cold end of the HRB. Therefore, like the above point (i), the heat recovery ratio χ decreases with increasing T_3.

The Figure 5(c) shows the overall efficiency of the bottoming cycle η_{rec} and the electric power output of the bottoming cycle. As for Eq.(3), it appears that, considering saturated cycles, the overall efficiency η_{rec} is always increasing with the evaporation pressure, despite the heat recovery ratio is decreasing. In the case of subcritical superheated cycles, it appears that superheating is generally useful for cycles with low evaporation pressure, while, for high evaporation pressures (>8 bar), saturated cycles show overall efficiency higher than superheated cycles with the same evaporation pressure. Finally, similar results have been obtained with supercritical cycles; it appears that, over a certain evaporation pressure, the overall efficiency decreases with the maximum temperature.

2.2 Influence of recuperation on the ORC cycle

The choice of a recuperative heat exchanger (RHE) in the bottoming ORC cycle is discussed here. Recuperation in the bottoming cycle has a limited influence on the overall efficiency of the bottoming cycle, η_{rec} . In fact, recuperation in the bottoming cycle improves the thermal efficiency of the bottoming cycle η_L but causes a reduction of heat recovery ratio χ, since the organic fluid that feeds the HRB is preheated in the regenerator. A comparison of the performance, with and without recuperation, is given in Figure 6 for a saturated cycle with ORC turbine inlet temperature of 150°C. It appears that with recuperator, the overall efficiency η_{rec} is a little higher. In general, it seems preferable the solution with recuperator that is characterized by a higher stack temperature and lower enthalpy of the organic fluid entering the condenser. In the interplay between heat rejection at the stack or at the condenser, the first choice appears preferable.

Figure 6 - Comparison between ORC cycles with and without recuperation. Saturated cycle, T_3=150°C.

Table 3- Thermodynamic parameters of working fluid

Figure 7 - Saturated cycles for toluene and MM.

2.3 Performance of the bottoming ORC with different fluids

The analysis of the choice of the working fluid on the bottoming cycle is given hereafter. The selected fluids for the comparison are: hexamethyldisiloxane (MM), octamethyltrisiloxane (MDM), decamethyl-tetrasiloxane (MD2M) and Toluene. Siloxanes are fluids composed of molecules containing alternate silicon and oxygen atoms in either a linear or a cyclic arrangement, usually

with two or three organic groups attached to each silicon atom. At ambient conditions, siloxanes are liquid and appear slightly viscous, odorless, and transparent [36]. Toluene, instead, is an aromatic hydrocarbon. Table 3 gives the main characteristics of the examined fluids, on the basis of their molecular complexity [37,38].

The comparison is carried out only for saturated cycle on the basis of the previous results. **Figure 8** shows the internal efficiency η_L, the heat recovery ratio χ and the overall efficiency of the bottoming ORC plant, η_{rec}, with the corresponding electric power output, $P_{e,ORC}$. It appears that the internal efficiency $\eta_L$is about the same for all the considered fluids, while there is a significant difference for the heat recovery ratio χ. This result can be justified by observing Figure 7 that shows the T-s diagrams of the cycles for toluene and MM, with the same evaporation temperature. It appears that the turbine exit temperature is lower for the cycle operated with toluene. Therefore, due to the recuperative heat exchanger, the feed liquid temperature to the HRB is lower for the toluene cycle than for MM cycle. This results in a lower stack temperature T_G for toluene than for MM.

In the case of the cycles operated by MDM and MD2M, Figure 8(b) shows that, like the cycle operated by MM, the recovery factor χ decreases with the evaporation temperature (that is the turbine inlet temperature) with values lower than MM and toluene. This determinates lower overall efficiency η_{rec} for MDM and MD2M cycles, as shown in Figure 8(c).

In conclusion, the analysis shows that toluene and MM guarantee the highest overall efficiency η_{rec} and power output, with a maximum of about 780 kW, reached by the cycle operated by toluene with evaporation pressure of 41 bar.

Figure 8-Comparison among MM, MDM, MD2M and Toluene for saturated cycles. Effect of ORC Turbine Inlet Temperature and evaporation pressure on a)η_L, b) χ and c) η_{rec} and electric power output.

2.4 Preliminary design of the ORC turbine

The choice of the thermodynamic points has a strong influence on the turbine design. To this purpose, it is necessary to introduce the volumetric expansion ratio, V_r, and the size parameter S_p as follows

$$V_r = \frac{\dot{V}_{out}}{\dot{V}_{in}}, \tag{7}$$

$$S_p = \frac{\sqrt{\dot{V}_{out}}}{\Delta h_{is}^{1/4}}, \quad (8)$$

where $\dot{V}_{in}$ and $\dot{V}_{out}$ are turbine inlet and outlet volume flows and Δh_{is} is turbine isentropic enthalpy drop. Volumetric ratio regards compressibility effects while size parameter is proportional to the turbine dimensions [31,39]. Due to the large molecular weight, ORC cycles are characterized by small turbine enthalpy drops Δh_{is} and large volumetric ratios V_r.

The evaluation of V_r and $S_p$can be done directly from the thermodynamic cycle and can be used for the estimation of the turbine efficiency, making use of efficiency maps that can be found in several works (see, e.g. [31, 39, 40]. Such maps allow us to verify if the hypotheses on the turbine isentropic efficiency assumed for thermodynamic calculations are acceptable or not.

Figure 9 – Volumetric expansion ratio and Size Parameter chart. Comparison between MM, MDM, MD2M and Toluene

Figure 10 – Chart of ORC electric power output vs. Volumetric ratio. Saturated cycles.

Figure 9 shows the chart of V_r vs. S_p for the examined fluids, considering saturated cycles. It appears that MDM and MD2M give very high values of V_r (>150) that cause unacceptable detriment of the turbine efficiency, even with high values of size parameter.

Figure 10 shows the estimated power output (considering $\eta_{is,t}$ constant and equal to the value given in Table 1) as a function of the volumetric ratio. In order to consider both plant performance and turbine design, it helps one to select a thermodynamic point able to reach the best tradeoff between ORC power output and volumetric ratio. It appears that at the same volumetric ratio, toluene gives better overall cycle efficiency than MM. In particular, it can be observed that, with evaporation pressure p_{ev}=10 bar, the volumetric ratio is 120 and the power output of the ORC plant is 700 kW, not far from the maximum of about 780 kW and, from Figure 9, the size parameter is about 0.22 m. From charts in [26] and [39],it can be shown that, for this point, the estimated isentropic efficiency is within the range 0.78-0.84, depending on the model adopted for estimation of the turbine losses. Therefore, the value of 0.8 assumed for the isentropic efficiency in the thermodynamic calculations can be considered acceptable for the aims of the present work. This result is in agreement with the assumptions of [27]. Then, the following thermo-economic analysis will be carried out for this design point. The performance of the combined cycle plant obtained under such hypotheses are given in Table 4 where are compared to the simple EFGT cycle.

346 **Table 4. Technical parameters and modeling results**

347 ## 3. THERMO-ECONOMIC ANALYSIS

348 A profitability assessment of the combined cycle EFGT+ORC as resulting from the previous
349 thermodynamic analysis, is proposed in this section with comparison to the simple EFGT cycle
350 (Table 4). The main advantage of the bottoming ORC is the increased electric conversion
351 efficiency, while the drawback is the higher upfront cost and lower heat available for cogeneration.
352 In the case of the simple EFGT, high temperature heat can be recovered (hot air exiting the turbine
353 at 394°C). Further thermal power is available from the intercooler heat exchanger (IC) for
354 compression intercooling, at a temperature of 110°C. However, this has been disregarded in the
355 thermo-economic assessment, since it may cause further complication of the plant layout and
356 operation because of the cold water needed to cool the compressed air at the prescribed temperature,
357 which could be difficult when, due to the variability of the heat demand, no heat is absorbed for
358 cogeneration. In the case of the combined cycle EFTG-ORC, the air exiting from the HRB is at
359 104°C, hence the cogeneration applications are only for low grade thermal energy demand (40 °C).
360 The different temperature of cogenerated heat with and without bottoming ORC and the
361 correspondent on site heat demand requirements represent the main key factors for the selection of
362 the most profitable cycle configuration.

363 In this analysis, a low grade thermal energy demand at 40 °C and a $\Delta T_{\min}$ of the heat exchanger
364 for cogeneration of 10°C are assumed, which means 60% and 90% of heat recovery respectively for
365 the two configurations. As in the previous plant configuration, useful heat could be recovered also
366 from the intercooler; however, the heat from intercooling is again neglected, for the same reasons
367 described above for the EFGT plant.

368 In this application, the profitability is assessed for the two scenarios of only electricity
369 generation and cogeneration of heat and power, and a sensitivity analysis to heat demand intensities
370 and heat selling prices is proposed. With the assumptions of Table 1 for hot air genset efficiency,
371 LHV and moisture content of biomass of 40% dm, and taking into account biomass storage losses
372 of 1%, the fuel consumption results of 25,694 t/yr. The proposed thermo-economic methodology is
373 described in [11]. The basic strategy of baseload operating mode and electricity fed into the grid is
374 here assumed, being this typology of CHP plants eligible for feed-in tariffs in the Italian energy
375 market [3, 46].

376

377 **Table 5.** Capex and opex costs assumptions

378

3.1 Costs assessment

The turn key costs are estimated by means of interviews and data collections from manufacturers of the selected technologies. In particular, the following sources have been considered: Saturn 20 Solar Turbines; Turboden for the ORC genset; personal elaboration from Areva and Koblitz data and literature references [41-43] for biomass storage, handling and conveyor systems; Uniconfort data [44] for biomass boiler, hot air genset and heat exchanger (max T of 800°C); civil works, grid connection, engineering, installation: personal estimates from interviews to operators of biomass fired ORC power plants in the 1-2 MWe size range and literature [45]. The heat distribution and delivery to final end users is excluded from the costs assessment, being this study mainly focused on the profitability of the bottoming ORC in comparison to the single cycle EFGT. The Capex and Opex cost items are summarized in Table 5. The annual O&M costs are assumed 4% of the turn key cost and the ash discharge are accounted for assuming unitary cost of 70 Eur/t ash. Personnel costs are respectively 244 and 268 kEur/yr, as resulting from unitary labour costs in Italy and data from plant operators [45] and manufacturers. The cost of biomass supply (included transport) is 50 Eur/t (17.5 Eur/MWh).

3.2 Energy revenues and financial assumptions

The financial appraisal of the investment is carried out assuming the following hypotheses: (i) 20 years of operating life; no 're-powering' throughout the 20 years; zero decommissioning costs; (ii) maintenance costs, fuel supply costs, electricity and heat selling prices held constant (in real 2015 values); (iii) duration of feed-in tariff for biomass electricity of 20 years (iv) capital assets depreciated using a straight line depreciation over 20 years; (v) cost of capital (net of inflation) equal to 5%, corporation tax neglected, no capital investments subsidies.

A baseload operation mode is assumed for the power plant, being all generated electricity sold to the grid at the feed-in electricity price available in the Italian framework [11, 46], which is 231 and 221 Eur/MWh respectively for CHP and only electricity, in the assumed power size range and considering the BAT for air emissions abatement, and use of agricultural by-products from local and sustainable supply chains [47]. The electricity generation is calculated assuming operating hours of 8,040 per year.

Figure 11. NPV (top) and IRR (bottom) of the investment as a function of the heat demand (hr/y)

3.3 Profitability assessment results

The profitability assessment results are reported in Figures 11 to 13 that show respectively the NPV and IRR as a function of: (i) the equivalent heat demand of the load, (ii) the heating selling price and (iii) the biomass supply cost. The sensitivity assessment of NPV and IRR on respect to these factors is carried out assuming starting values of 3,000 hours/year for the equivalent heat demand, 40 Eur/MWh for the heat selling price, temperature of heat demand of 40°C and biomass supply cost of 50 Eur/t. As it can be seen, the option with bottoming ORC is more profitable than the baseline case of only EFGT, because of the higher electric efficiency and electricity revenues. On the contrary, the latter option results profitable only at high heat demand and heating selling price levels. This is mainly due to the low electric efficiency of the cycle, despite the relatively low investment cost (having assumed low TIT and no regenerator). The heat demand typology is certainly a key factor when comparing the profitability of the two cycles. In particular, if the low grade temperature available from the ORC is not compatible with the heat requirement of the load (i.e. steam demand), and at high thermal energy demand levels (above 5,000 hr/year) and/or high heat selling prices (above 60 Eur/MWh), the EFGT option results more profitable than the EFGT+ORC one (where the low T heat would be discharged and not useful for the load). This is shown in Figure 14, which reports the increment of NPV of the bottoming ORC option as a function of temperature of heat demand, and at different heat demand and heating selling price levels. As can be seen, at H_T of 5,000 hour/yr and P_T of 80 Eur/MWh, (case 4 of Fig 14) the EFGT+ORC option is less profitable than the EFGT. The biomass supply cost is another important parameter, as appears in Fig 13. However, it has almost the same influence on the two configurations, and makes the EFGT profitable at biomass costs below 60 Eur/t, while the EFGT+ORC cycle remains profitable even at higher biomass supply costs.

Figure 12. NPV (top) and IRR (bottom) of the investment as a function of the heat selling price

Further relevant aspects are the maintenance and personnel costs, which could be decreased when locating the plant at the premises of industrial facilities, or the business model options to operate the plant and maximize the performance in combination with active demand response, load following or energy storage. For this reason, further studies on operational flexibilities, part load performances and different operational strategies (heat/electricity driven and option to switch off the ORC in presence of high temperature heat demand) should be deepened to increase the accuracy of the study. This would be particularly relevant if the generous feed-in tariffs here assumed (Italian subsidy framework) were not available and the electricity revenues would be estimated on the basis

444 of the avoided costs of electricity from on site generation and the sales of excess energy to the grid
445 at market prices.
446
447 **Figure 13.** NPV (top) and IRR (bottom) of the investment as a function of the biomass supply cost
448
449 **Figure 14 -** Increment of NPV with bottoming ORC as a function of the temperature of heat
450 demand; case 1: h_t=3,000 h/yr – P_t=40 Eur/MWh; Case 2: h_t=5,000 h/yr – P_t=40 Eur/MWh; Case 3:
451 h_t=3,000 h/yr – P_t=80 Eur/MWh; Case 4: h_t=5,000 h/yr – P_t=80 Eur/MWh

452 ## 4. CONCLUSIONS

453 A thermodynamic analysis has been carried out on a combined cycle composed by an EFGT and a
454 bottoming ORC cycle. The parametric analysis regards exclusively the bottoming cycle where
455 different turbine inlet temperature and evaporation pressure are explored in order to compare
456 saturated, superheated and supercritical cycles. The results of the thermodynamic analysis show
457 that, in the case of subcritical cycles, superheating causes a decrease of the power output, hence the
458 adoption of saturated cycle is mandatory. Similar results have been obtained in the case of
459 supercritical cycles that show how the overall efficiency of the bottoming cycle decreases when
460 increasing the turbine inlet temperature, thus suggesting that the turbine inlet conditions should be
461 chosen in proximity of the critical point.
462 The comparison among different fluids (MM, MDM, MD2M and Toluene) has shown that Toluene
463 provides the best efficiency in this specific application, mainly due to a better heat recovery ratio,
464 χ, that occurs due to the relatively high temperature (394°C) of the heat available at the turbine
465 exit.
466 In order to take in consideration the design of the ORC on the plant performance, the size parameter
467 S_p and the volumetric ratio V_r have been examined.. The results show that the volume ratio
468 increases with the evaporation pressure leading to high values of Mach number in the turbine
469 expansion and, consequently, low isentropic efficiency. The turbine design has been selected on the
470 basis of the maps of efficiency given in [25] and [38]and consequently a saturated cycle with
471 evaporation pressure of 10 bar can be chosen, in agreement with the choice proposed by [26].
472 Finally, the financial appraisal of the EFGT plant with and without bottoming ORC allows drawing
473 relevant considerations about the technical and economic key factors that influence the profitability
474 of bottoming ORC cycle coupled to biomass fired EFGT. The combined cycle EFGT+ORC results
475 more profitable than the simple EFGT option, because of its higher electric efficiency. However, in
476 case of high temperature of heat demand, high thermal energy demand levels, and/or high heating
477 selling prices, the EFGT configuration without bottoming ORC could be the most profitable one.

Future researches regard the optimization of operation strategies, taking into account energy demand patterns, part load efficiencies, heat to electricity output ratio flexibility, real time electricity selling prices, storage options, active demand response approaches and broad integration into smart grids and energy hubs.

ACNOKNWLEDGEMENTS

The work has been partly supported by the Research Project PONA3_O0372: "High education to Innovative Energy Conversion Processes (F-PRINCE). The financial support of the PON02_00323_3588749 "SMART ENERGY BOXES (SEB)" is also gratefully acknowledged.

NOMENCLATURE

Symbol	Quantity	SI Unit
A	Surface area	m^2
h	Enthalpy	kJ/kg
p	Pressure	bar
T	Temperature	°C
MW	Molecular weight	kg/kmol
$\dot{m}$	Mass flow	kg/s
$\dot{V}$	Volume flow	m^3/s
P	Power	kW
P_T	Thermal energy selling price	Eur/MWh
H_T	Equivalent heat demand	hour/year
$\dot{Q}$	Heat Power	kW
S_p	Size parameter	m
V_r	Volumetric ratio	
Greek		
η	Efficiency	
χ	Heat recovery ratio	
Subscrips		
a	air	
v	vapour	
cr	critical	
in	inlet	

out	outlet
e	electric
ev	evaporation
av	available
is	isentropic
HR	Heat Rejected
L	Low (bottoming cycle)
rec	recuperator

Acronyms

IC	Intercooler
HRB	Heat Recovery Boiler
RHE	Recuperative Heat Exchanger
EFGT	External Fired Gas Turbine
IRR	Internal Rate of Return
MM	hexamethyldisiloxane
MDM	octamethyltrisiloxane
MD2M	decamethyl-tetrasiloxane
NPV	Net Present Value
ORC	Organic Rankine Cycle
TIT	Turbine Inlet Temperature

489

490

REFERENCES

[1] Decision 406/2009/EC of the European Parliament and of the Council of 23 April 2009

[2] Directive 2009/28/EC of the European Parliament and of the Council of 23 April 2009

[3] Pantaleo A, Candelise C. Bauen A, Shah N (2014): ESCO business models for biomass heating and CHP: case studies in Italy, Renewable and Sustainable Energy Reviews, 30, 237-253

[4] Yan J, Eidensten L. Status and perspective of externally fired gas turbines. J Propul Power 2000;16(4).

[5] Cocco, D., Deiana, P., & Cau, G. (2006). Performance evaluation of small size externally fired gas turbine (EFGT) power plants integrated with direct biomass dryers. Energy, 31(10-11), 1459–1471. doi:10.1016/j.energy.2005.05.014

[6] Ferreira, A. C. M., Nunes, M. L., & Martins, L. A. S. B. (2012). A Review of Stirling Engine Technologies applied to micro-Cogeneration Systems. In Proceedings of ECOS 2012 (pp. 338–399). Perugia, Italy.

[7] Kong, X. (2004). Energy efficiency and economic feasibility of CCHP driven by Stirling engine. Energy Conversion and Management, 45(9-10), 1433–1442. doi:10.1016/j.enconman.2003.09.009

[8] Dong, L., Liu, H., & Riffat, S. (2009). Development of small-scale and micro-scale biomass-fuelled CHP systems – A literature review. Applied Thermal Engineering, 29(11-12), 2119–2126. doi:10.1016/j.applthermaleng.2008.12.004

[9] Chacartegui, R., Sánchez, D., Muñoz, J. M., & Sánchez, T. (2009). Alternative ORC bottoming cycles for combined cycle power plants. Applied Energy, 86(10), 2162–2170. doi:10.1016/j.apenergy.2009.02.016

[10] Pantaleo A, Ciliberti P, Camporeale S, Shah N (2015) Thermo-economic assessment of small scale biomass CHP: steam turbines vs ORC in different energy demand segments, Proceedings of 7th International Conference on Applied Energy – ICAE 2015, Abu Dhabi, March 28-31/2015

[11] Pantaleo, A. M., Camporeale, S. M., & Shah, N. (2013). Thermo-economic assessment of externally fired micro-gas turbine fired by natural gas and biomass□: Applications in Italy. Energy Conversion and Management, 75, 202–213.

[12] Pantaleo, A. M., Camporeale, S., & Shah, N. (2014). Natural gas–biomass dual fuelled microturbines: Comparison of operating strategies in the Italian residential sector. Applied Thermal Engineering, 71(2), 686–696. doi:10.1016/j.applthermaleng.2013.10.056

[13] Camporeale S, Turi F, Torresi M, Fortunato B, Pantaleo A, Pellerano A (2015) Part load performances and operating strategies of a natural gas-biomass dual fuelled microturbine for CHP operation, Journal for Engineering for Gas Turbines and Power, 137(12) (13 pp) doi: 10.1115/1.4030499

[14] Baina, F., Malmquist, A., Alejo, L., & Fransson, T. H. (2015). Effect of the fuel type on the performance of an externally fired micro gas turbine cycle. Applied Thermal Engineering, 87, 150–160. doi:10.1016/j.applthermaleng.2015.04.042

[15] Ferreira SB, Pilidis P, Macro AR. The use of biomass fuels in gas turbine combined cycles: gasification vs. externally fired cycle. RIO 3dWorld Climate & Energy Event. Brazil: Rio de Janeiro; December 1–5 2003.

[16] Evans RL, Zaradic AM. Optimization of a wood-waste-fuelled, indirectly fired gas turbine cogeneration plant. Bioresour Technol 1996;57:117–26.

[17] Eidensten L, Yan J, Svedberg G. Biomass externally fired gas turbine cogeneration. J Eng Gas Turb Power. Trans ASME 1996;118:604–9.

[18] Wolf J, Barone F, Yan J. Performance analysis of evaporative biomass air turbine cycle with gasification for topping combustion. J Eng Gas Turb Power. Trans ASME 2002;12(4):757.

[19] Eidensten L, Yan J, Svedberg G. Biomass externally fired gas turbine cogeneration. J Eng Gas Turb Power. Trans ASME 1996;118.

[20] Iora, P., & Silva, P. (2013). Innovative combined heat and power system based on a double shaft intercooled externally fired gas cycle. Applied Energy, 105, 108–115. doi:10.1016/j.apenergy.2012.11.059

[21] Al-attab KA, Zainal ZA. Performance of high-temperature heat exchangers in biomass fuel powered externally fired gas turbine systems. Renewable Energy 2010;35:913–20.

[22] Kautz M, Hansen U. The externally-fired gas-turbine (EFGT-cycle) for decentralized use of biomass. Appl Energy 2007;84:795–805.

[23] Barsali S; Giglioli R; Ludovici G; Poli D. (2011). A MICRO COMBINED CYCLE PLANT FOR POWER GENERATION FROM SOLID BIOMASS: COUPLING EFMGT AND ORC. In 19th European Biomass Conference. Berlin: ETA-WIP,

551 [24] Bagdanavicius, A., Sansom, R., Jenkins, N., & Strbac, G. (2012). Economic and
552 exergoeconomic analysis of micro GT and ORC cogeneration systems. In ECOS 2012 (pp. 1–
553 11).

554 [25] Leonardo Pierobon, Tuong-Van Nguyen, Andrea Mazzucco, Ulrik Larsen and Fredrik Haglind
555 "Part-Load Performance of a Wet Indirectly Fired Gas Turbine Integrated with an Organic
556 Rankine Cycle Turbogenerator", Energies 2014, 7, 8294-8316; doi:10.3390/en7128294

557 [26] Camporeale S, Ciliberti P, Torresi M, Fortunato B, Pantaleo A (2015), Externally fired micro
558 gas turbine and ORC bottoming cycle: optimal biomass/natural gas CHP configuration for
559 residential energy demand, Proceedings of ASME Turbo Expo, Montreal, Canada, June 15-
560 19/2015

561 [27] C M Invernizzi, P Iora, and R Sandrini. "Biomass combined cycles based on externally fired
562 gas turbines and organic Rankine expanders" Proc. IMechE Vol. 225 Part A: J. Power and
563 Energy, 1066-1075

564 [28] Meinel, C. Wieland, H. Spliethoff. "Effect and comparison of different working fluids on a
565 two-stage organic Rankine cycle (ORC) concept". Applied Thermal Engineering 63 (2014)

566 [29] G. David, F. Michel, L. Sanchez. "Waste heat recovery projects using Organic Rankine Cycle
567 technology – Examples of biogas engines and steel mills applications." Geneve 2011- World
568 Engineer's Convention

569 [30] Hung TC, Shai TY, Wang SK. A review of organic Rankine cycles (ORCs) for the recovery of
570 low-grade waste heat. Energy 1997;22(7):661–7.

571 [31] E. Macchi, "The choice of working fluid: the most important step for a successful Organic
572 Rankine Cycle (and an efficient turbine)" [Tech. Presentation], in: 2nd Int. Seminar on ORC
573 Power Systems, De Doelen, Rotterdam, NL, 2013.

574 [32] H. Chen, D.Yogi Goswami, E.K. Stefanakos. "A review of thermodynamic cycles and working
575 fluids for the conversion of low-grade heat". ELSEVIER, 2010

576 [33] http://www.asimptote.nl/software/cycle-tempo (accessed on March 22nd, 2015)

577 [34] Karsten Kusterer, René Braun, Dieter Bohn. "Organic Rankine cycle working fluid selection
578 and performance analysis for combined application with a 2 MW class industrial gas turbine".
579 Proceedings of ASME Turbo Expo -2014, June 16 – 20, 2014, Düsseldorf, Germany

580 [35] B.F. Tchanche, G. Papadakis, G. Lambrinos, A. Frangoudakis. "Fluid selection for a low-
581 temperature solar organic Rankine cycle". Applied Thermal Engineering 29 (2009) 2468–2476

582 [36] Uris, M., Linares, J. I., & Arenas, E. (2014). Techno-economic feasibility assessment of a
583 biomass cogeneration plant based on an Organic Rankine Cycle. Renewable Energy, 66, 707–
584 713.

585 [37] A. Uusitalo, J. Honkatukia, T. Turunen-Saaresti, J. Larjola, P. Colonna. “Suitability of
586 siloxanes for a mini ORC turbogenerator based on high-speed technology”

587 [38] C. He, C. Liu, H. Gao, H. Xie, Y. Li, S. Wu, J. Xu. “The optimal evaporation temperature and
588 working fluids for subcritical organic Rankine cycle”. ELSEVIER, 2012.

589 [39] P. Klonowicz, F. Heberle, M. Preißinger, D. Brüggemann, Significance of loss correlations in
590 performance prediction of small scale, highly loaded turbine stages working in Organic
591 Rankine Cycles, Energy, Volume 72, August 2014,Pages 322-330

592 [40] A. Lazzaretto, G. Manente, A New Criterion to Optimize ORC Design Performance using
593 Efficiency Correlations for Axial and Radial Turbines, International Journal of
594 Thermodynamics (IJoT), Vol. 17 (No. 3), pp. 173-181, 2014

595 [41] Arvay, P., Muller, M. R., & Ramdeen, V. (2011). Economic Implementation of the Organic
596 Rankine Cycle in Industry. ACEEE Summer Study on Energy Efficiency in Industry, 12–22.

597 [42] Pantaleo, A., & Shah, N. (2013). The Logistics of Bioenergy Routes for Heat and Power, in
598 “Biofuels - Economy, Environment and Sustainability.” (F. Zhen, Ed.). intech.

599 [43] personal information from Areva

600 [44] Uniconfort www.uniconfort.com

601 [45] personal information from Fiusis Srl, www.fiusis.com

602 [46] Legislative Decree 28/2011 (in Italian) ‘Attuazione della direttiva 2009/28/CE sulla
603 promozione dell’uso dell’energia da fonti rinnovabili’

604 [47] Ministry Decree 6-7-2012 on renewable energy subsidy levels in Italy

605 [48] J.H. Horlock, Combined Power Plants, Pergamon Press, 1992

606 [49] Esen H, Inalli M., Esen M, (2006) Technoeconomic appraisal of a ground source heat pump
607 system for a heating season in eastern Turkey, Energy Conversion and Management, 47(9-10),
608 1281-1297

609 [50] Kaabechea A, Belhamela M, Ibtiouenb R (2011) Techno-economic valuation and optimization
610 of integrated photovoltaic/wind energy conversion system, Vol 85(10) Solar Energy,
611 doi:10.1016/j.solener.2011.06.032

612 [51] Esen M, Tahsin Yuksel T (2013) Experimental evaluation of using various renewable energy
613 sources for heating a greenhouse, Energy and Buildings, 65, 340-351

614 [52] Utlu, Z., & Hepbasli, A. (2008). Thermoeconomic analysis of energy utilization in the
615 residential–commercial sector: An application. Building and Environment,43(5), 896-904.

616 [53] Marzband M., Sumper A., Domínguez-García J. L., Gumara-Ferret R., "Experimental
617 Validation of a Real Time Energy Management System for Microgrids in Islanded Mode Using
618 a Local Day-Ahead Electricity Market and MINLP", Energy Conversion and Management,
619 Vol. 76, pp. 314-22, 2013.

620 [54] Gu, W., Wu, Z., Bo, R., Liu, W., Zhou, G., Chen, W., & Wu, Z. (2014). Modeling, planning
621 and optimal energy management of combined cooling, heating and power microgrid: A
622 review. International Journal of Electrical Power & Energy Systems, 54, 26-37.

623 [55] Dong, L., Liu, H., & Riffat, S. (2009). Development of small-scale and micro-scale biomass-
624 fuelled CHP systems–A literature review. Applied thermal engineering, 29(11), 2119-2126.

625

626

627 **LIST OF FIGURES**

628

654

655

656 **FIGURES**

657

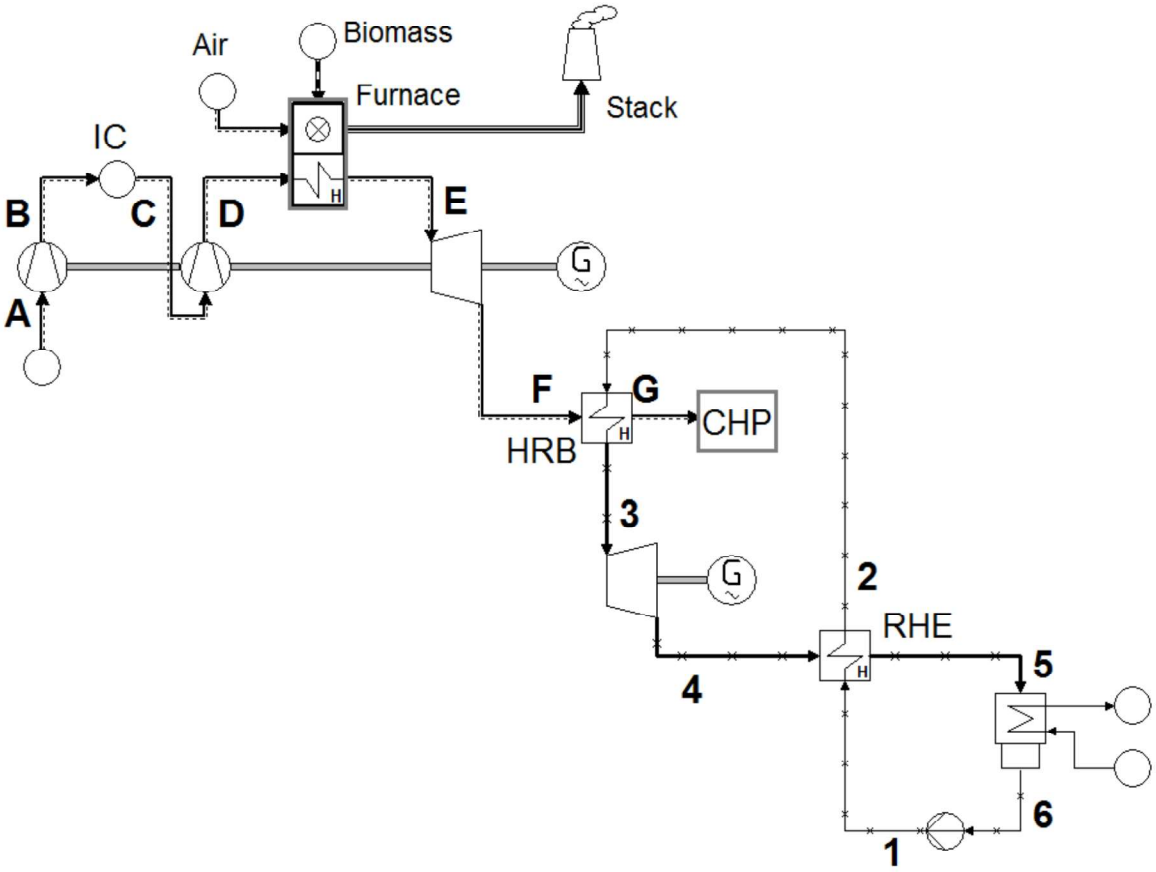

658

659 **Figure 1 –** EFGT+ORC Combined Cycle Plant Layout

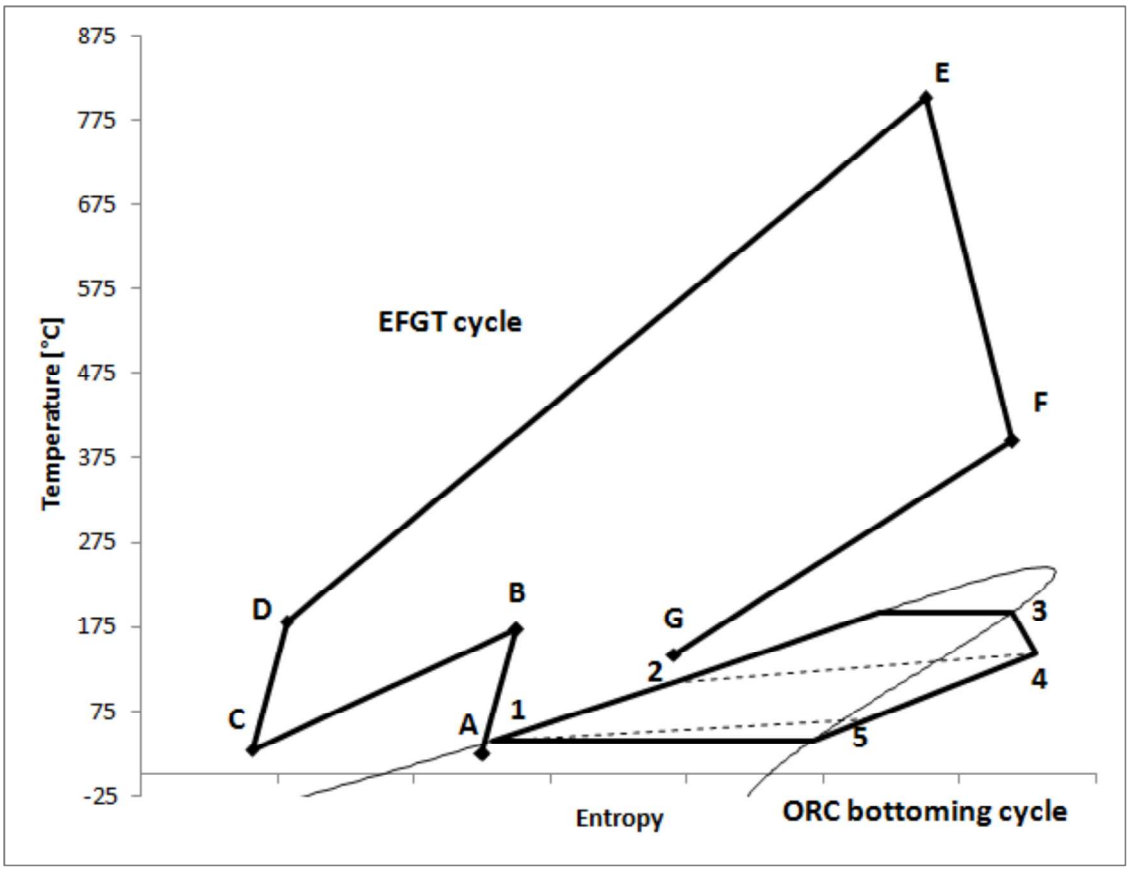

660

661 **Figure 2 -** T-s chart. EFGT-ORC Combined Cycle.

662

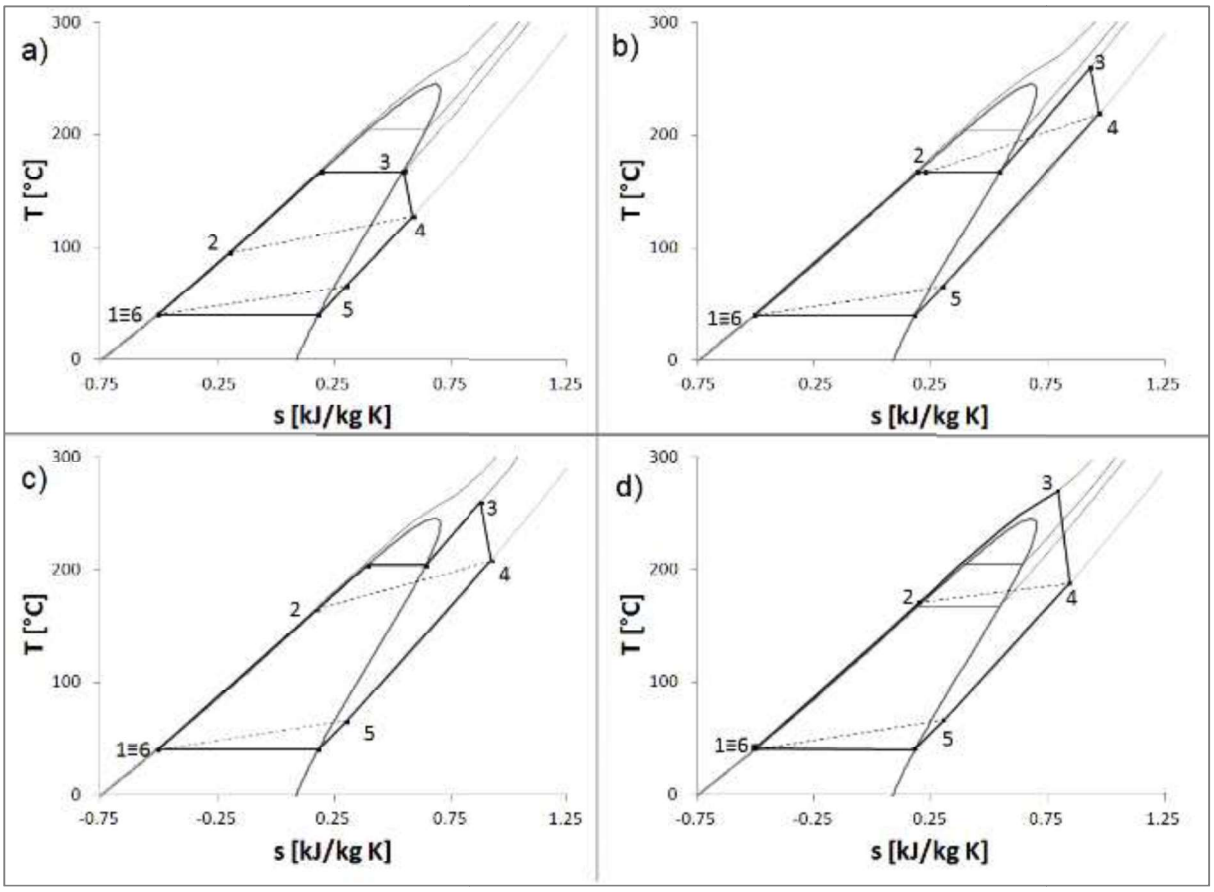

Figure 3 – T-s chart for some examined cases: a) p_{ev}=5 bar, saturated; b) p_{ev}=5 bar, T_3=260°C; c) p_{ev}=10 bar, T_3=260°C; d) supercritical cycle p_{ev}=25 bar, T_3= 270°C

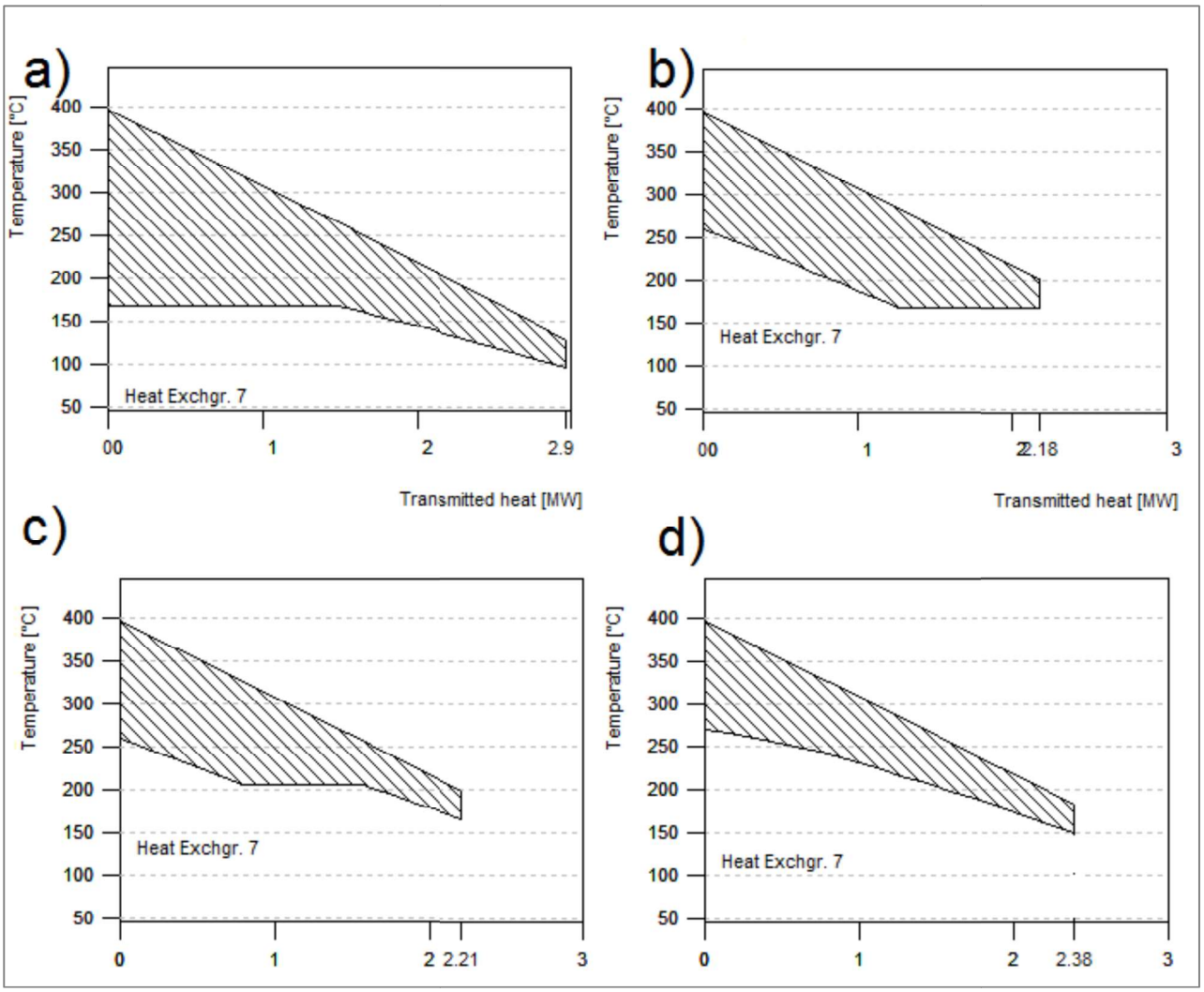

667

668 **Figure 4** –T-Q diagrams for the HRB. Cases (a) to (d).

669

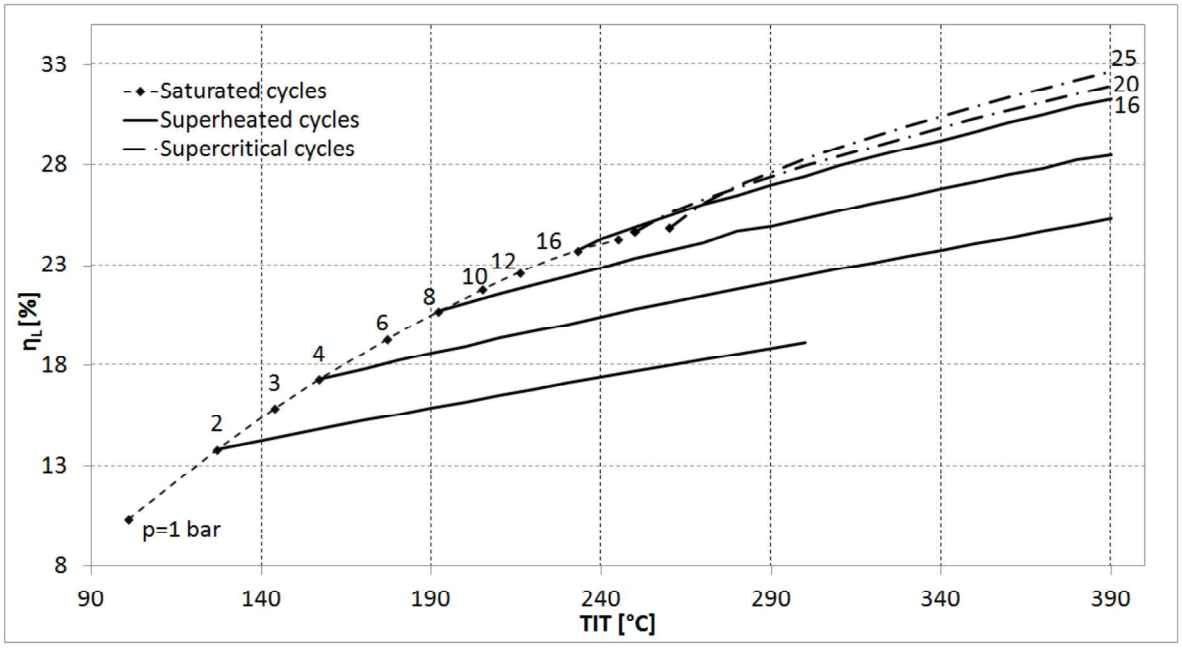

670

671 Figure 5 (a)-

672

673

674

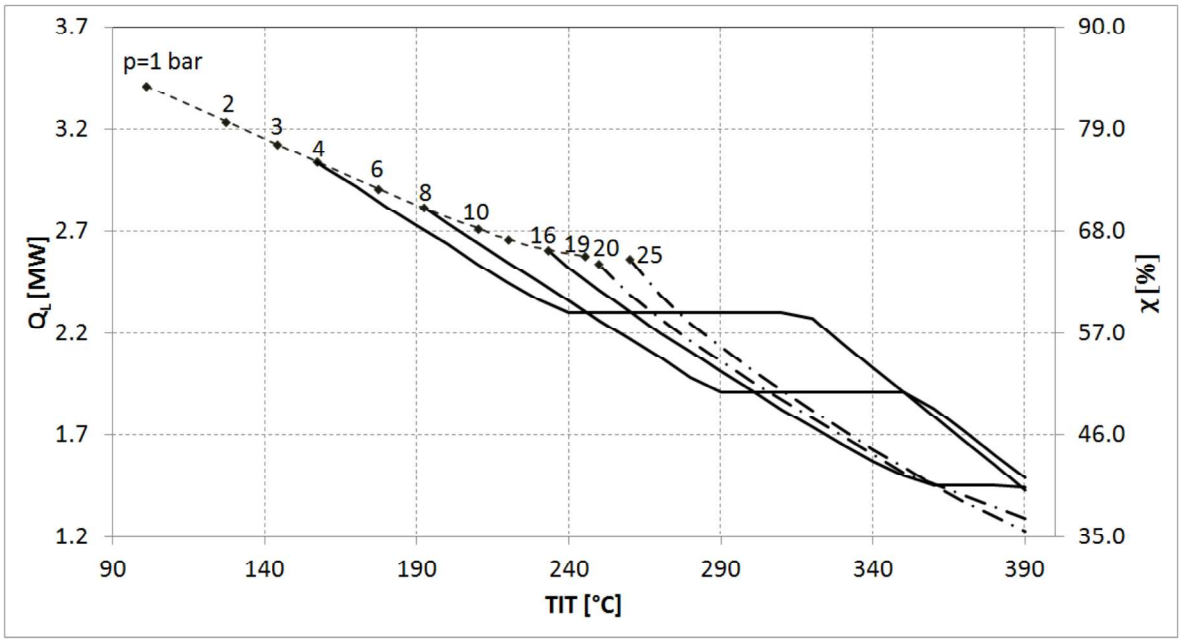

675

676 Figure 5 (b)

677

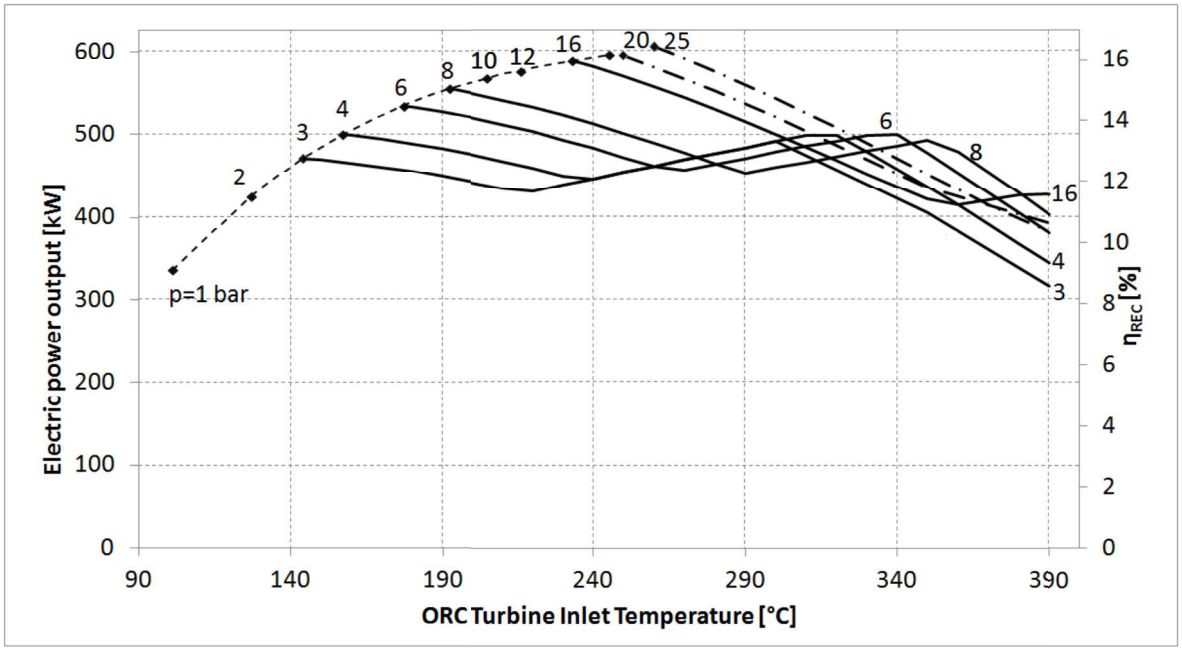

Figure 5 (c)

Figure 5- Effect of Turbine Inlet Temperature and Evaporation Pressure on a) internal ORC cycle thermal efficiency, η_L ; b) heat exchanged in the HRB and heat recovery ratio; c) electric power output and overall efficiency of the ORC cycle, η_{rec}, for subcritical (1 to 19 bar) and supercritical (20 to 25 bar) cycles

686

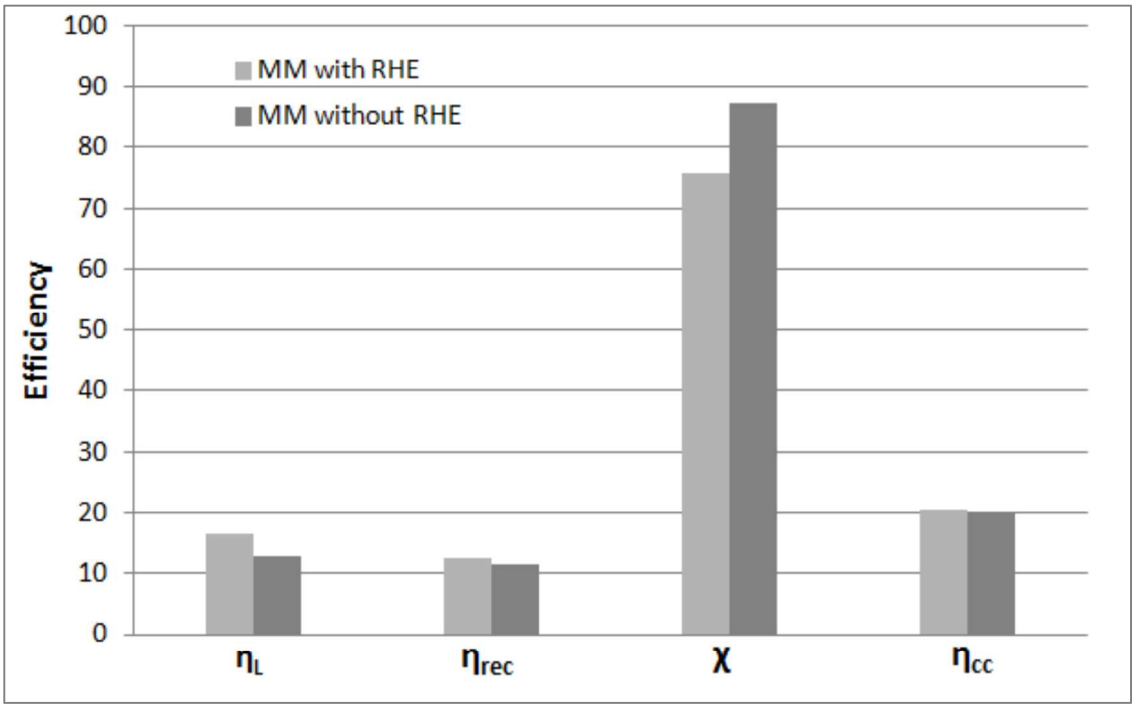

687

688 **Figure 6 -** Comparison between ORC cycles with and without recuperation.

689 Saturated cycles, T_3=150°C.

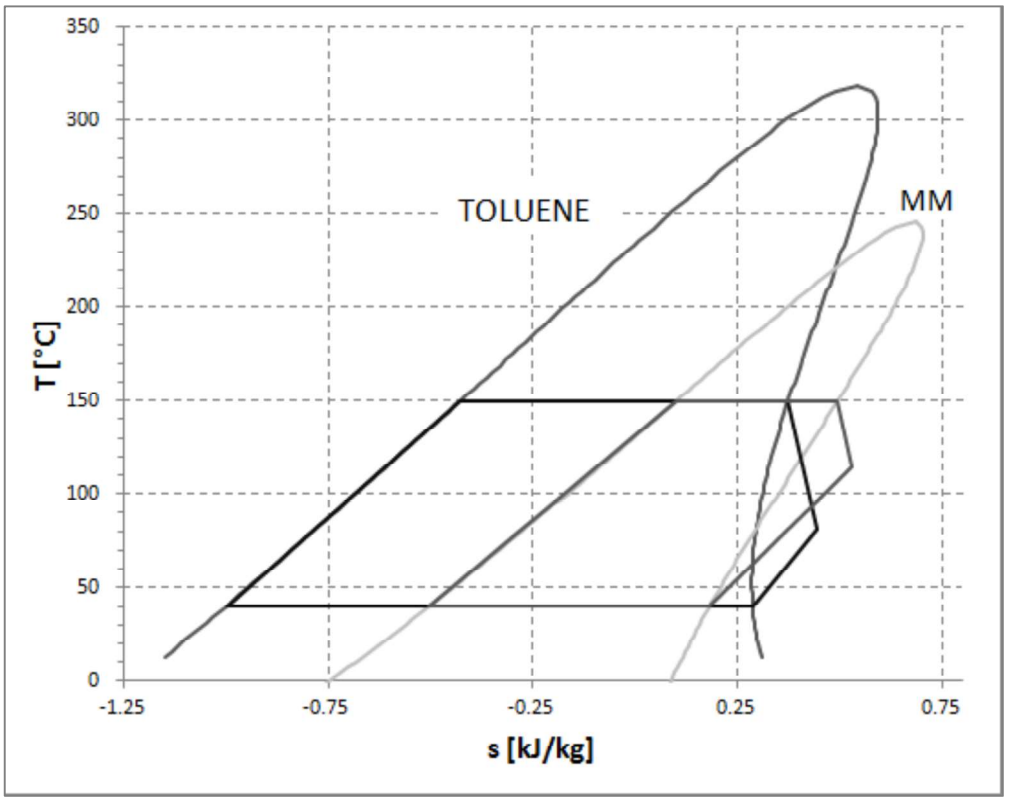

690

691 **Figure 7 -** Saturated cycles for toluene and MM.

692

693

694

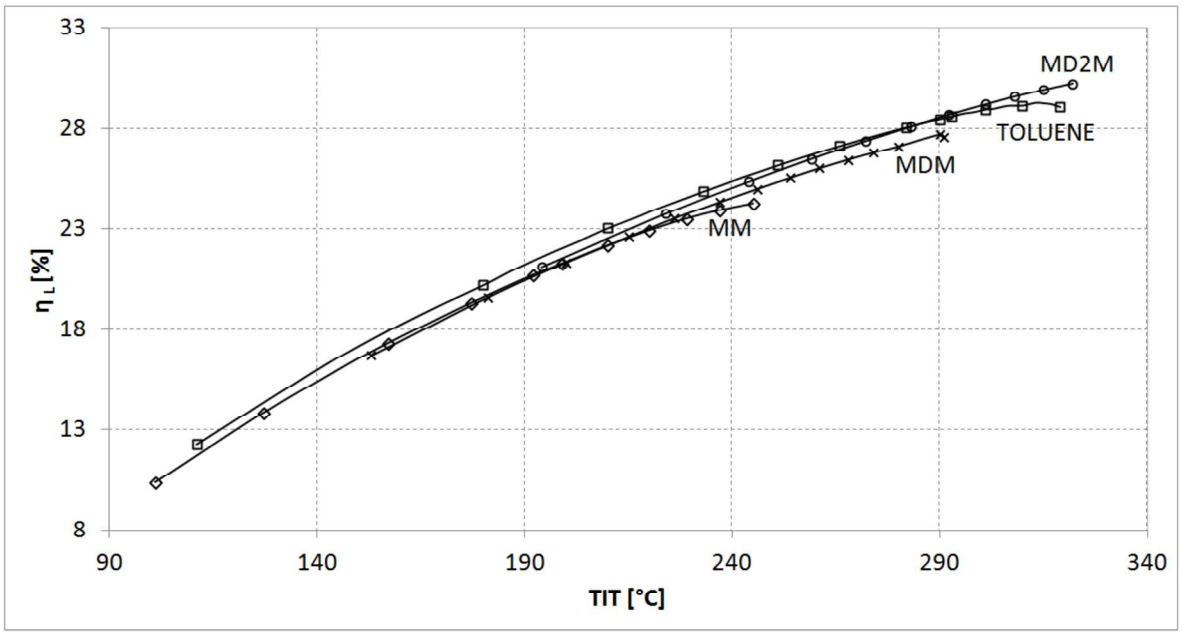

695

696 Figure 8 (a)

697

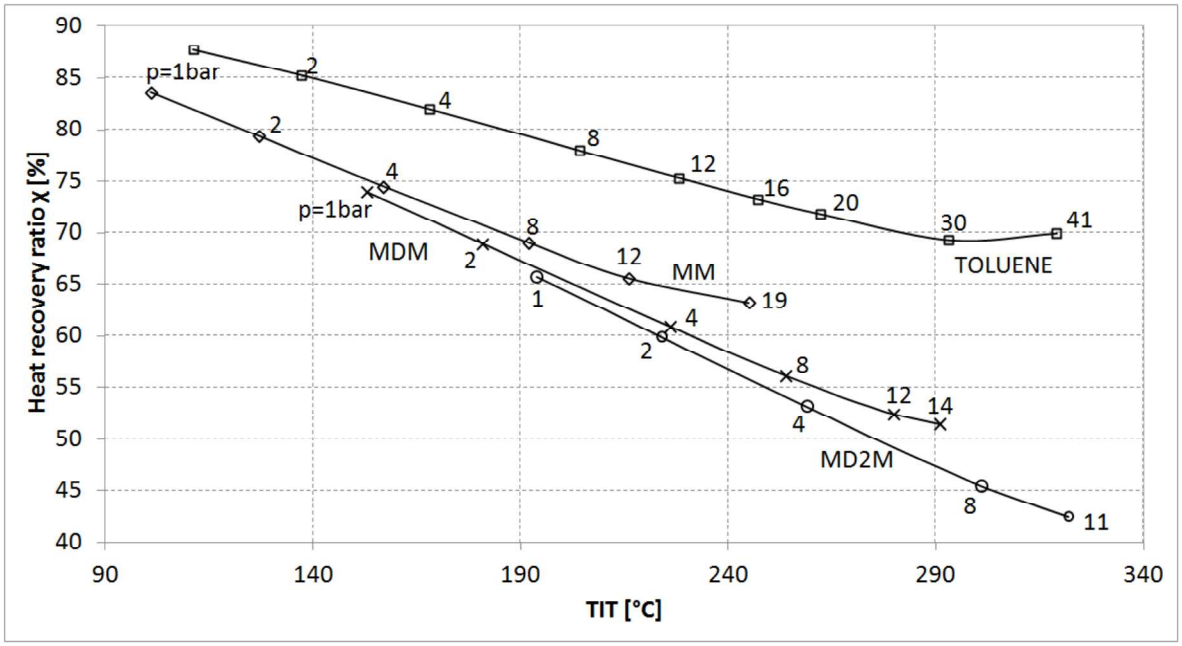
Heat recovery ratio χ [%]
TIT [°C]
90
85
80
75
70
65
60
55
50
45
40
90
140
190
240
290
340
p=1bar
2
4
8
12
16
20
30
41
TOLUENE
p=1bar
2
4
8
12
19
MM
MDM
2
1
4
2
8
12
14
4
MD2M
8
11

Figure 8 (b)

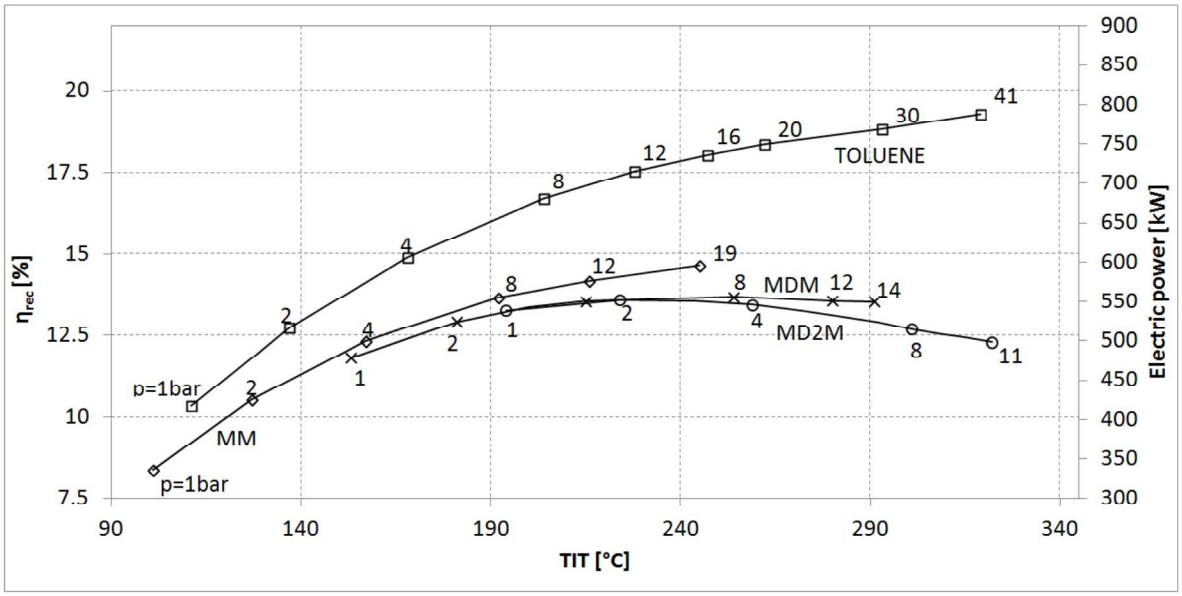

Figure 8 (c)

Figure 11-Comparison among MM, MDM, MD2M and Toluene for saturated cycles. Effect of ORC Turbine Inlet Temperature and evaporation pressure on a) η_L, b) χ and c) η_{rec} and electric power output.

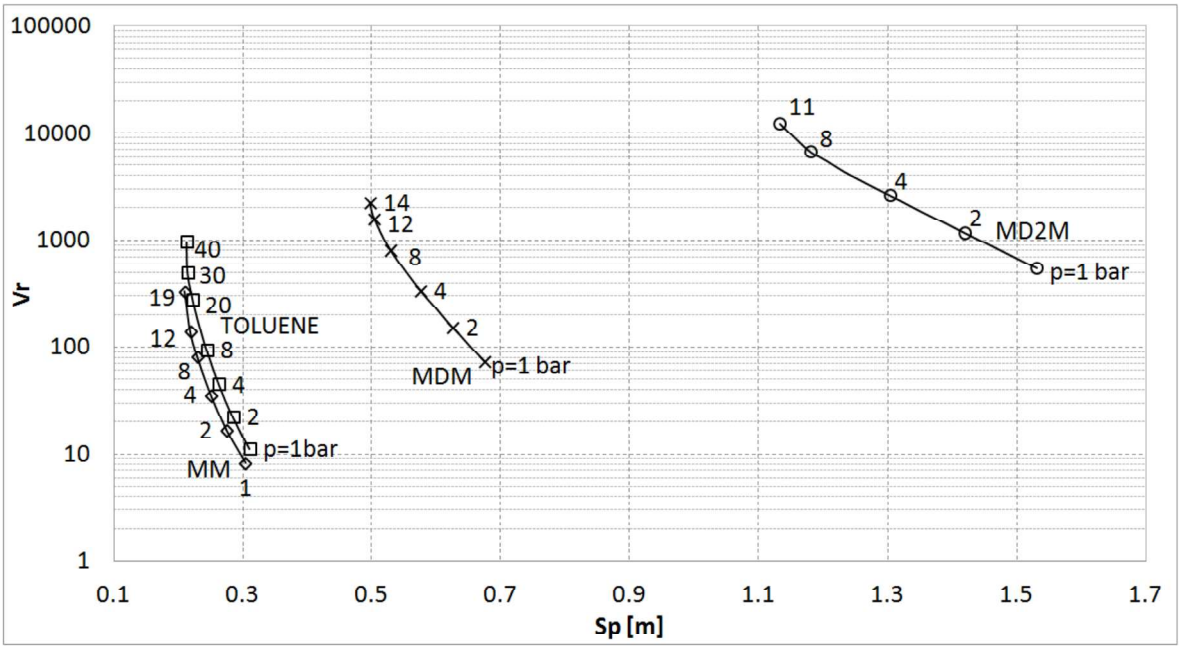

710

711

712 **Figure 9 –** Volumetric expansion ratio and Size Parameter chart. Comparison between MM, MDM,

713 MD2M and Toluene

714

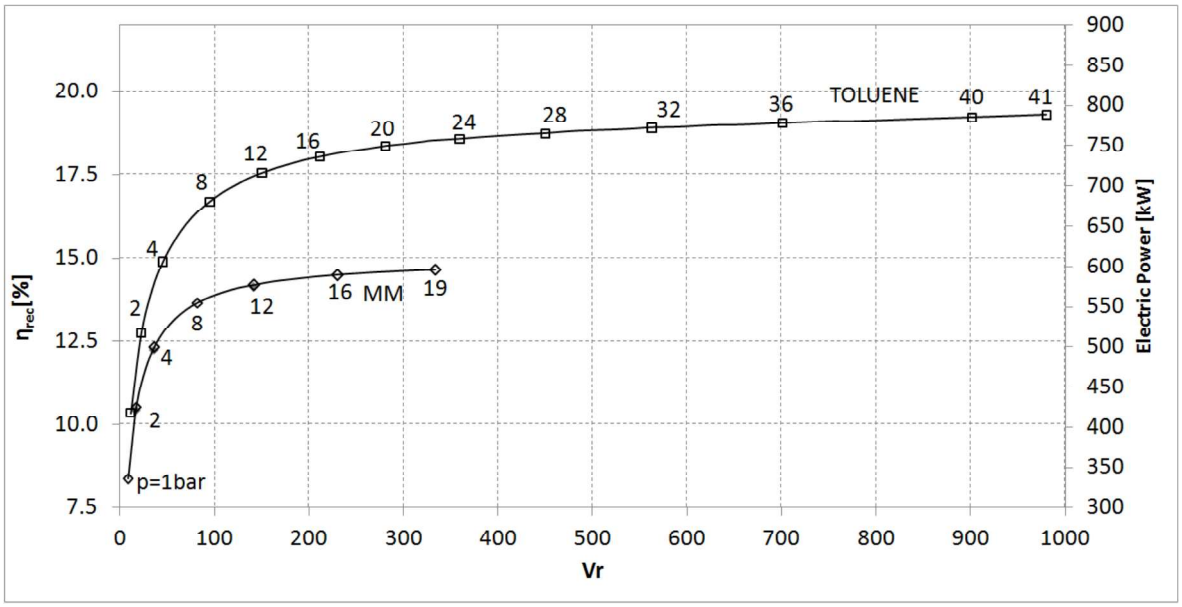

Figure 10 – Chart of ORC electric power output vs. Volumetric ratio. Saturated cycles.

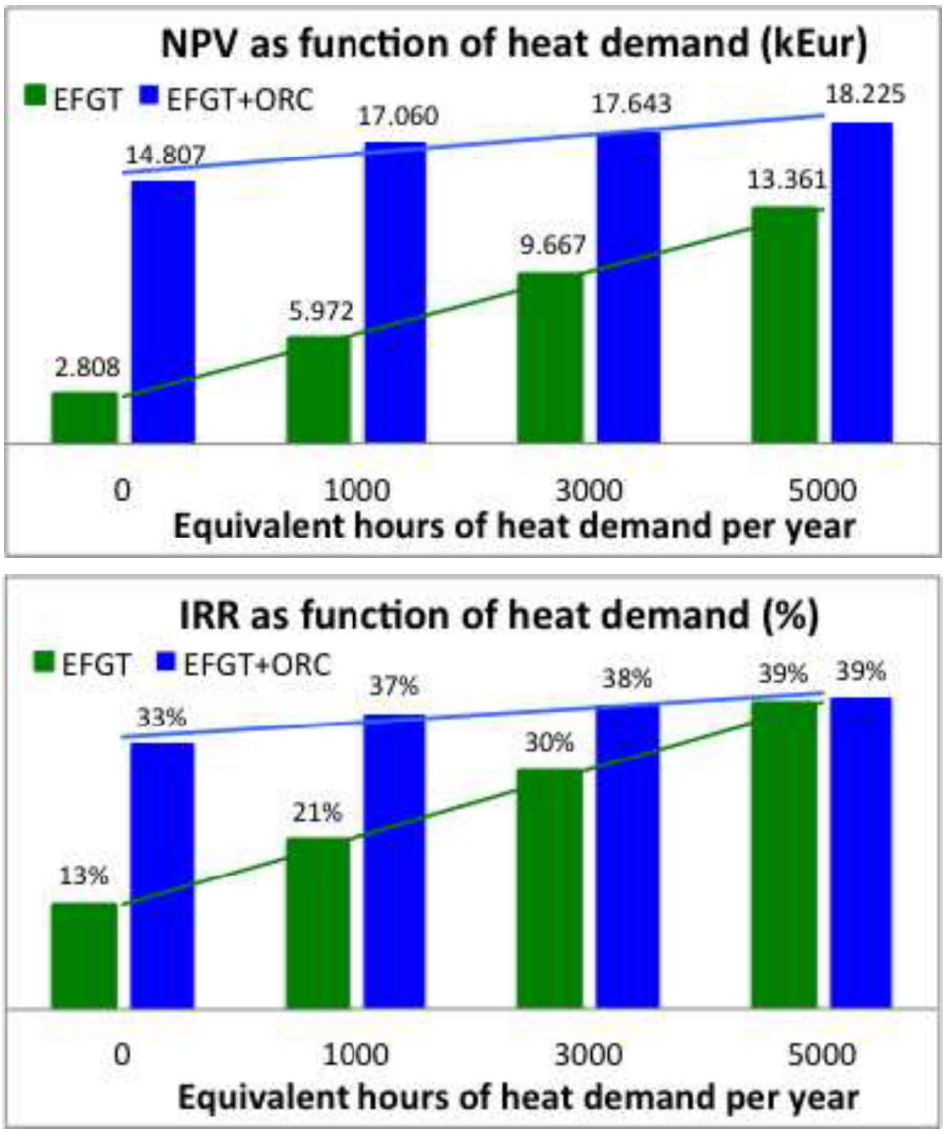

Figure 11. NPV (top) and IRR (bottom) of the investment as a function of the heat demand H_T (hour/y)

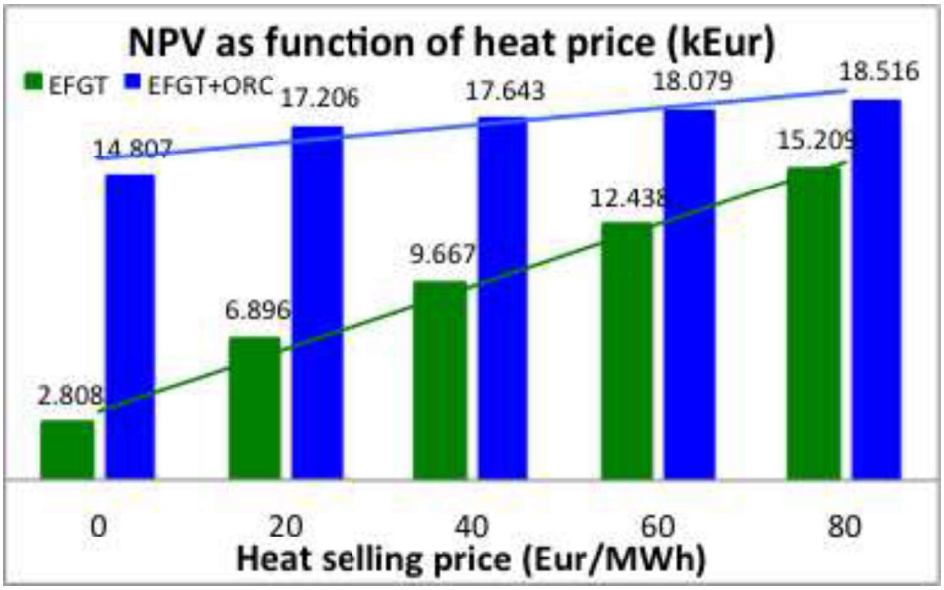

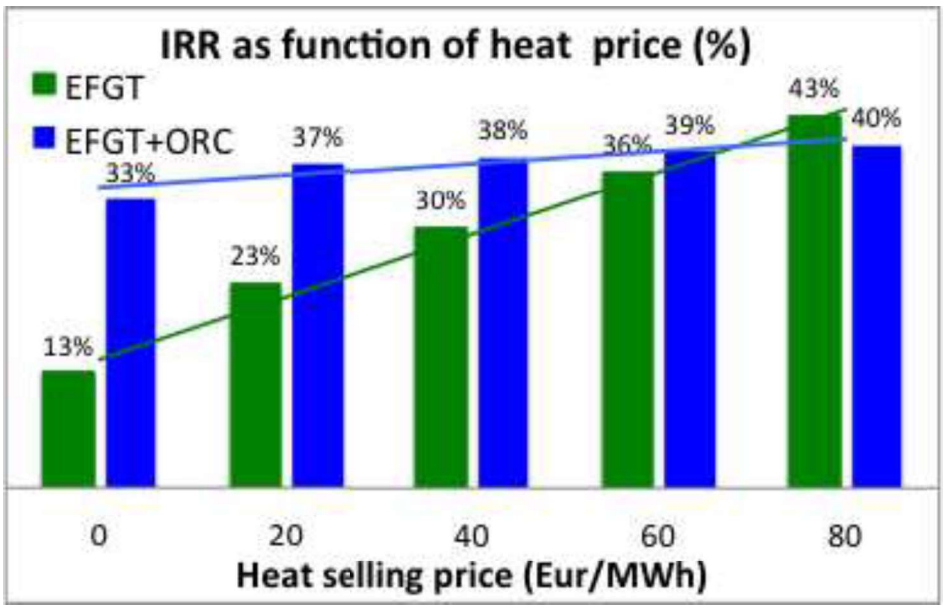

Figure 12. NPV (top) and IRR (bottom) of the investment as a function of the heat selling price P_T

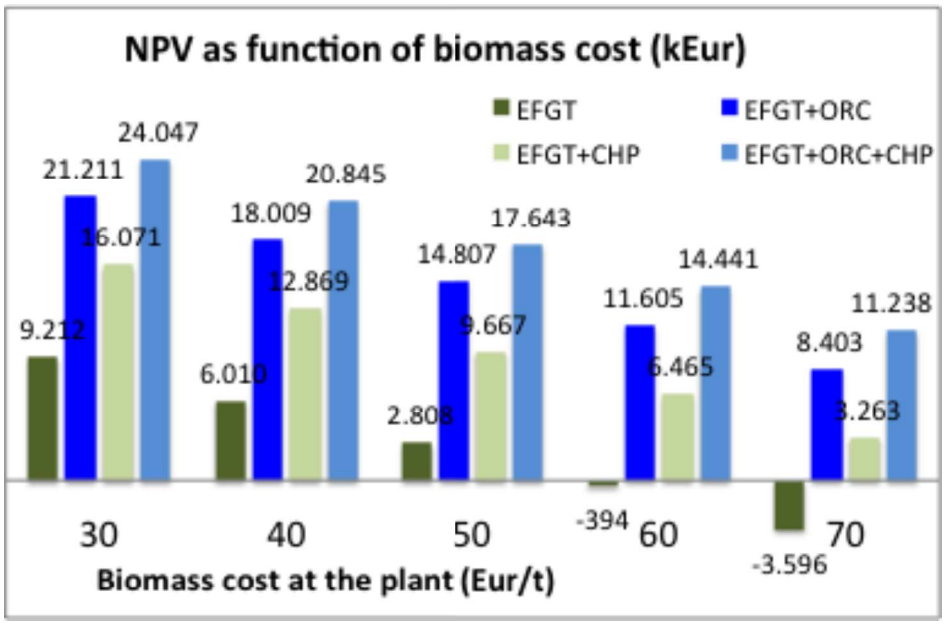

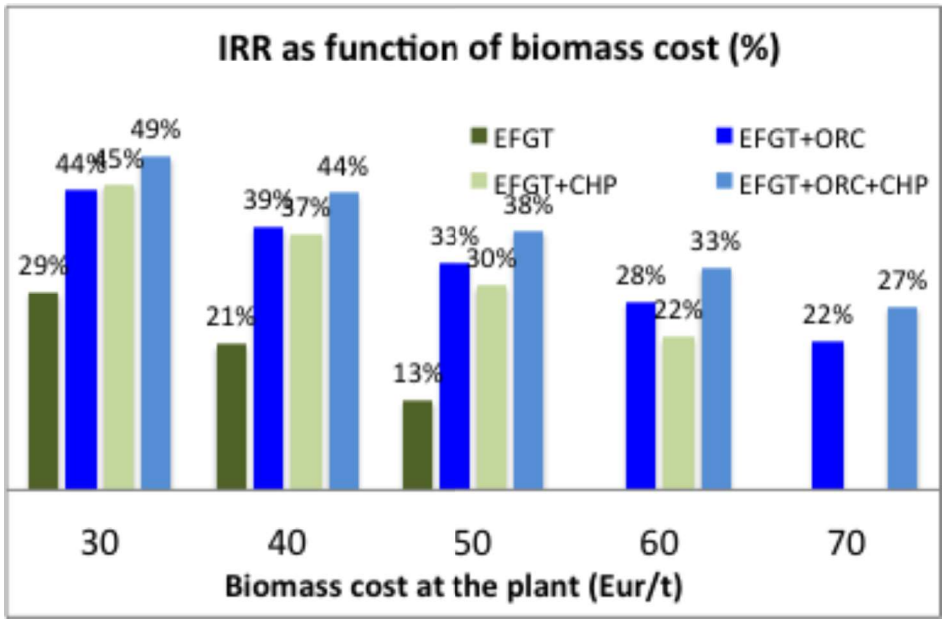

Figure 13. NPV (top) and IRR (bottom) of the investment as a function of the biomass supply cost (40% moisture content)

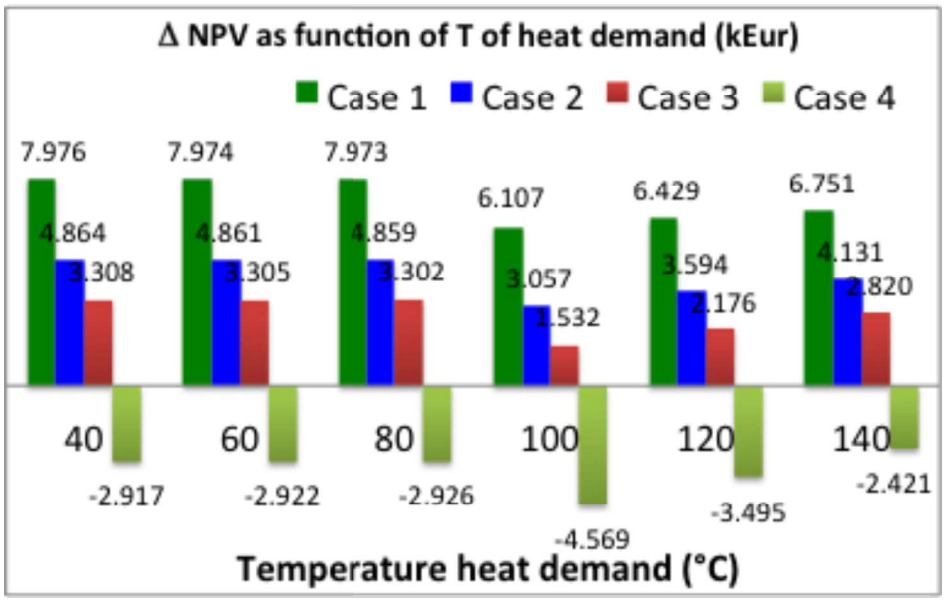

Figure 14 - Increment of NPV with bottoming ORC as a function of the temperature of heat demand; case 1: H_T=3,000 h/yr – P_T=40 Eur/MWh; Case 2: H_T=5,000 h/yr – P_T=40 Eur/MWh; Case 3: H_T=3,000 h/yr – P_T=80 Eur/MWh; Case 4: H_T=5,000 h/yr – P_T=80 Eur/MWh

LIST OF TABLES

TABLES

Table 1 –Main calculation hypotheses for the EFGT cycle

Description	**Value**	**Units**
Overall Pressure ratio	12	
Turbine Inlet Temperature	800	°C
Biomass mass flow	1	kg/s
Lower Heating Value, LHV	10,300	kJ/kg
Air factor λ	1.3	
Biomass Furnace efficiency	0.80	
Isentropic compressor efficiency	0.85	
Mechanical compressor efficiency	0.98	
Turbine Isentropic efficiency	0.85	
Turbine mechanical efficiency	0.98	
Electric generator efficiency	0.95	

Table 2- Basic assumed value for ORC calculation

Description	**Value**
Pump Isentropic Efficiency	0.75
Pump Mechanical Efficiency	0.96
Turbine isentropic Efficiency	0.80
Turbine Mechanical Efficiency	0.96
Electric generator efficiency	0.95
ΔT_{min} in the RHE	25°C
ΔT_{min} in the HRB	33°C
Condenser temperature	40°C

774 **Table 3-** Thermodynamic parameters of working fluid

775

Organic Fluid	Type	p_{cr} [bar]	T_{cr} [°C]	MW [kg/kmol]
Toluene	Isentropic	41.06	318.6	92.14
MM	Dry	19.39	245.6	162.37
MDM	Dry	14.15	290.9	236.53
MD2M	Dry	11.79	326.2	310.69

782

783

784

785

786

787 **Table 4. Technical parameters and modeling results**

Parameter	Unit	EFGT	EFGT +ORC
Electric power output (ISO) P_N	kW	1,383	2,083
Auxiliary consumption (in % P_N)	%	5	6
Thermal Power output (for CHP)	kW	4,083	963
Gas temperature (for CHP)	°C	394	104
Net-electric efficiency (ISO)	%	15.3	23.0

788

789

790

791

792 **Table 5. Capex and opex costs assumptions**

Description	EFGT	EFGT+ ORC
Turn Key cost (kEur)	3,500	4,700
of which:		
Gas Turbine	1,200	1,200
ORC genset	-	1,200
Biomass furnace	1,000	1,000
Heat exchanger	600	600
Civil works	500	500
Grid connection	100	100
Engine, develop., insurances	100	100
Unit upfront cost (kEur/kWe)	2.53	2.26
Opex (included fuel) (kEur/yr)	1,722	1,771

793

794

795